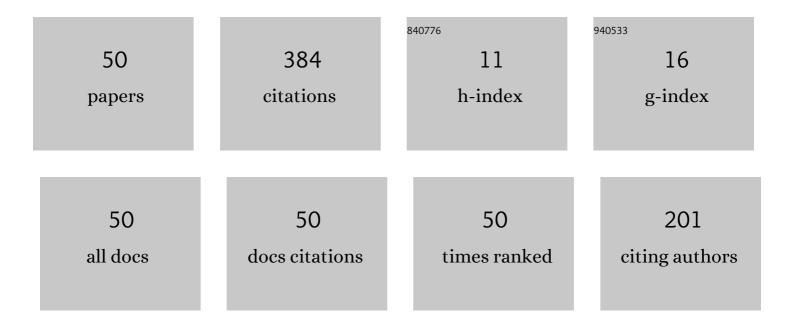
Boris P Sobolev

List of Publications by Year in descending order

Source: https://exaly.com/author-pdf/5580842/publications.pdf Version: 2024-02-01



#	Article	IF	CITATIONS
1	The universal defect cluster architecture of fluorite-type nanostructured crystals. CrystEngComm, 2022, 24, 3762-3769.	2.6	7
2	Full quasi-system "from LaF3 to LuF3―as a combination of 14 binary systems of lanthanide trifluorides with maximal chemical proximity. Journal of Solid State Chemistry, 2022, 312, 123163.	2.9	7
3	Displacements in the Cationic Motif of Nonstoichiometric Fluorite Phases Ba1â^'xRxF2+x as a Result of the Formation of {Ba8[R6F68–69]} Clusters: III. Defect Cluster Structure of the Nonstoichiometric Phase Ba0.69La0.31F2.31 and Its Dependence on Heat Treatment. Crystals, 2021, 11, 447.	2.2	6
4	High-temperature chemistry of Y, La and lanthanide trifluorides in RF3–R'F3 systems. Part 1. Chemical classification of systems. Journal of Solid State Chemistry, 2021, 298, 122079.	2.9	3
5	High-temperature chemistry of Y, La and lanthanide trifluorides in RF3–R'F3 systems. Part 3. Phase composition of the studied systems. Journal of Solid State Chemistry, 2021, 298, 122080.	2.9	2
6	High-temperature chemistry of Y, La and lanthanide trifluorides in RF3–R'F3 systems. Part 2. Phase diagrams of the studied systems. Journal of Solid State Chemistry, 2021, 298, 122078.	2.9	2
7	Refinement of the Congruently Melting Composition of Nonstoichiometric Fluorite Crystals Ca1-xYxF2x (x = 0.01–0.14). Crystals, 2021, 11, 696.	2.2	1
8	Nanostructured Crystals of Fluorite Phases Sr1–xRxF2+x (R Are Rare-Earth Elements) and Their Ordering. 16: Defect Structure of the Nonstoichiometric Phases Sr1–xRxF2+x (R = Pr, Tb–Yb) As Grown. Crystallography Reports, 2020, 65, 560-565.	0.6	5
9	75LiF + 25SmF3 Eutectic Composite and Ionic Conductivity of SmF3 near the Polymorphic α–β Transition. Crystallography Reports, 2020, 65, 468-472.	0.6	2
10	Effect of Heat Treatment in a СF4 Atmosphere on the Ion-Conductive Properties of Hot-Pressed 95 mol % CeF3 × 5 mol % SrF2 Ceramics. Crystallography Reports, 2019, 64, 105-109.	0.6	3
11	Fluorine-Ionic Conductivity of Superionic Conductor Crystals Na0.37Tb0.63F2.26. Crystallography Reports, 2019, 64, 626-630.	0.6	3
12	Growth of Sm1–ÂySryF3–Ây (0 < y ≤0.31) Crystals and Investigation of Their Properties. Crystallograph Reports, 2019, 64, 488-495.	^{IY} 0.6	2
13	Nanostructured Crystals of Fluorite Phases Sr1–ÂxRxF2Â+Âx (R Are Rare-Earth Elements) and Their Ordering. 14: Concentration Dependence of the Defect Structure of Nonstoichiometric Phases Sr1–ÂxNdxF2Â+Âx As Grown (x = 0.10, 0.25, 0.40, 0.50). Crystallography Reports, 2019, 64, 216-221.	0.6	2
14	Anisotropy of Ionic Conductivity of TbF3 Crystals. Crystallography Reports, 2019, 64, 621-625.	0.6	6
15	Crystal Growth and Thermal Conductivity of the Congruently Melting Solid Solution Cd0.77Sr0.23F2. Inorganic Materials, 2019, 55, 495-499.	0.8	8
16	Nanostructured Crystals of Fluorite Phases Sr1–ÂxRxF2Â+Âx (R Are Rare-Earth Elements) and Their Ordering. 13: Crystal Structure of SrF2 and Concentration Dependence of the Defect Structure of Nonstoichiometric Phase Sr1–ÂxLaxF2Â+Âx As Grown (x = 0.11, 0.20, 0.32, 0.37, 0.47). Crystallography Reports, 2019, 64, 41-50.	0.6	8
17	Growth of \$\${ext{N}}{{{ext{d}}}_{{{ext{d}}}_{{{ext{l}}; - ;y}}}{ext{Eu}}_{y}^{{{ext{2}} + }}{{{ext{3}}; - ;y}}}\$ Single Crystals with Tysonite-Type (LaF3) Structure and Investigation of the Concentration Dependence of Some Their Properties. Crystallography Reports, 2019. 64, 354-359.	0.6	3
18	Nanostructured Crystals of Fluorite Phases Sr1–ÂxRxF2Â+Âx (R Are Rare-Earth Elements) and Their Ordering. 15. Concentration Dependence of the Defect Structure of As Grown Nonstoichiometric Phases Sr1–ÂxRxF2Â+Âx (R = Sm, Gd). Crystallography Reports, 2019, 64, 873-878.	0.6	2

#	Article	IF	CITATIONS
19	Nanostructured Crystals of Fluorite Phases Sr1 – xR x F2 + x and Their Ordering: 12. Influence of Structural Ordering on the Fluorine-Ion Conductivity of Sr0.667R0.333F2.333 Alloys (R = Tb or Tm) at Their Annealing. Crystallography Reports, 2018, 63, 121-126.	0.6	5
20	Anisotropy of the Mechanical Properties of TbF3 Crystals. Crystallography Reports, 2018, 63, 96-103.	0.6	5
21	Growth of Fluorite Solid Solution Crystals in the Ternary SrF2–BaF2–LaF3 System and Investigation of Their Properties. Crystallography Reports, 2018, 63, 1015-1021.	0.6	2
22	Increase in the Fluorine-Ion Conductivity of Single Crystals of Tysonite-type CeF3 Superionic Conductor by Substituting Polarized Cd2+ Ions for Ce3+ Ions. Crystallography Reports, 2018, 63, 769-773.	0.6	4
23	Synthesis of Nonstoichiometric Samarium Fluoride SmF2 + x. Crystallography Reports, 2018, 63, 774-779.	0.6	2
24	Thermal Expansion of EuF2 + x Single Crystals and Their Thermal Stability. Crystallography Reports, 2018, 63, 614-620.	0.6	3
25	Ternary crystals Sr1â^'y Eu yâ^'x 2+Eu x 3+F2+x of fluorite phases with a variable europium valence and their thermal conductivity (50–300 K). Crystallography Reports, 2017, 62, 411-415.	0.6	5
26	Ionic conductivity of ScF3 single crystals (ReO3 type). Crystallography Reports, 2016, 61, 270-274.	0.6	6
27	Thermophysical characteristics of Pb0.679Cd0.321F2 solid-solution crystals. Crystallography Reports, 2015, 60, 111-115.	0.6	7
28	Nanostructured crystals of fluorite phases Sr1 â^' x R x F2 + x (R Are Rare Earth Elements) and their ordering: 10. Ordering under spontaneous crystallization and annealing of Sr1 â^' x R x F2 + x Alloys (R) Tj ETQo	0 0 ۵.6 gBT	∕O v erlock 10
29	Thermophysical characteristics of Ca1â~'x Sr x F2 solid-solution Crystals (0 ≤ ≤). Crystallography Reports, 2015, 60, 116-122.	0.6	21
30	Electrical and thermal conductivities of congruently melting single crystals of isovalent M 1 â^' x M′xF2 solid solutions (M, M′ = Ca, Sr, Cd, Pb) in relation to their defect fluorite structure. Crystallography Reports, 2015, 60, 532-536.	0.6	9
31	Thermophysical characteristics of EuF2.136 crystal. Crystallography Reports, 2015, 60, 740-743.	0.6	7
32	Growth of MgF2 optical crystals and their ionic conductivity in the as-grown state and after partial pyrohydrolysis. Crystallography Reports, 2014, 59, 928-932.	0.6	6
33	Nanostructured crystals of fluorite phases Sr1 â^' x R x F2 + x and their ordering: 9. The defect crystal and real structure of quenched fluorite phases Sr1 â^' x Ce x F2 + x (x = 0–0.5). Crystallography Reports, 2014, 59, 14-21.	0.6	8
34	Growth and magneto-optical properties of Na0.37Tb0.63F2.26 cubic single crystal. Crystallography Reports, 2014, 59, 718-723.	0.6	25
35	Anion conductivity of a Ce0.95Gd0.05O0.075F2.85 solid electrolyte. Inorganic Materials, 2014, 50, 513-518.	0.8	4
36	Nanostructured crystals of fluorite phases Sr1â^'x R x F2+x and their ordering: VIII. Imperfect crystal structure of Sr0.71Ce0.29F2.29. Crystallography Reports, 2013, 58, 678-681.	0.6	6

BORIS P SOBOLEV

#	Article	IF	CITATIONS
37	Coloring elimination in Sr1 â^' x Ce x F2 + x crystals in the visible spectral range during growth from melt. Crystallography Reports, 2013, 58, 755-759.	0.6	4
38	Nanostructured crystals of fluorite phases Sr1 â^' x R x F2 + x (R are rare-earth elements) and their ordering: IV. Study of the optical transmission spectra in the 2–17-μm wavelength range. Crystallography Reports, 2010, 55, 122-126.	0.6	12
39	Growth and some properties of Ce3+-doped LiYbF4 single crystals. Crystallography Reports, 2010, 55, 324-327.	0.6	2
40	Growth of congruently melting Ca0.59Sr0.41F2 crystals and study of their properties. Crystallography Reports, 2010, 55, 518-524.	0.6	30
41	Single crystals of the fluorite nonstoichiometric phase Eu 0.916 2+ Eu 0.084 3+ F2.084 (conductivity,) Tj ETQq1 1	0.78431	4 ₁ gBT /Ove
42	Nanostructured crystals of fluorite phases Sr1 â^' x R x F2 + x (R are rare earth elements) and their ordering: 5. A study of the ionic conductivity of as-grown Sr1 â^' x R x F2 + x crystals. Crystallography Reports, 2010, 55, 662-667.	0.6	19
43	Calculation of the Refractive Indices of M 1-x R x F2+x Crystals (M = Ca, Sr, Ba, Cd, Pb; R are Rare Earth) Tj ETQq1	1 0.78431 0.6	4 rgBT /Ov
44	Effect of heat treatment in HF atmosphere on the optical and electrical properties of BaF2 ceramics. Inorganic Materials, 2009, 45, 1188-1192.	0.8	5
45	Nanostructured crystals of fluorite phases Sr1 â [^] x R x F2 + x (R are rare-earth elements) and their ordering. I. Crystal growth of Sr1 â [^] x R x F2 + x (R = Y, La, Ce, Pr, Nd, Sm, Gd, Tb, Dy, Ho, Er, Tm, Yb, and) Tj ETQq2	1 d.0. 7843	3 ⊵4 rgBT /⊂
46	Defect structure and ionic conductivity of Ca1 â^' x Sc x F2 + x (0.02 ≤ ≤0.15) single crystals. Crystallography Reports, 2009, 54, 572-583.	0.6	4
47	Nanostructured crystals of fluorite phases Sr1 â^ x R x F2 + x (R = Y, La-Lu) and their ordering: Part III. A study of the refractive indices. Crystallography Reports, 2009, 54, 603-608.	0.6	24
48	The magnetocaloric effect in high-spin paramagnetic rare-earth fluorites. Materials Chemistry and Physics, 2007, 105, 62-66.	4.0	15
49	UV and VUV spectroscopic study of Na0.4Y0.6F2.2 crystals doped with rare-earth ions. Optics and Spectroscopy (English Translation of Optika I Spektroskopiya), 2006, 101, 571-581.	0.6	5
50	Investigation of multicomponent fluoride optical materials in the UV spectral region: I. Single crystals of Ca1â^'x R xF2+x (R = Sc, Y, La, Yb, Lu) solid solutions. Crystallography Reports, 2006, 51, 1009-1015.	0.6	12